**UCRL-89356 Rev 1**
**Preprint**

# Interaction of a Stream of Dielectric Spheres in an Electric Field in a High Vacuum

C.D. Hendricks
K. Kim

This paper was published in
The Institute of Electrical and Electronics Engineers
Transactions on Industrial Applications
May/June 1985

July 1984

Lawrence Livermore National Laboratory

# INTERACTION OF A STREAM OF DIELECTRIC SPHERES IN AN ELECTRIC FIELD IN A HIGH VACUUM*

Charles D. Hendricks
Lawrence Livermore National Laboratory
P.O. Box 5508
Livermore, California 94550

and

Kyekyoon Kim
Department of Electrical Engineering
University of Illinois
Urbana, Illinois 61801

## ABSTRACT

The interaction of a stream of dielectric spheres in an electric field in a high vacuum is investigated both theoretically and experimentally. This investigation is motivated by an attempt to detect fractional electric charges which might exist in matter, namely, a search for isolated quarks in matter. The theoretical analysis is intended to pinpoint the basic interaction mechanism by which a stream of dielectric spheres becomes destabilized in an electric field. One important result of this analysis is a suggested method by which the destabilizing forces can be eliminated. The experiments performed are intended to study the behavior of a stream of uniform liquid drops in an electric field in a high vacuum. It is seen from these experiments that the deflections of any two drops in the stream with charges differing by one electronic charge is the same except for the effects of some destabilizing forces.

*This work was performed under the auspices of the U.S. Department of Energy by Lawrence Livermore National laboratory under contract No. W-7405-Eng-48.

## I. INTRODUCTION

Several theoretical papers have been published indicating the possibility of the existence of fractional electric charges in matter. Fairbank and his co-workers at Stanford have reported experimental data which are indicative of the presence of fractional charges on superconducting niobium spheres.[1] A number of other experiments have been in progress for some time to search for fractional charges in other materials than niobium. Hagstrom, Hirsch, and Hendricks have used techniques of generating a stream of uniform liquid drops whose trajectories pass vertically through a constant electric field between two parallel vertical plates.[2] If the behavior of each of the drops is independent, the deflection of the drops as they pass through the electric field is a direct measure of the electric charge on the drops. In effect, this constitutes a charge spectrometer, a device for obtaining the charge spectrum of a stream of uniform mass particles.

A simplified schematic diagram of the experimental arrangement is shown in Fig. 1. The trajectories of drops with net charge in integer numbers of electrons are shown as dashed curves in the diagram with the trajectory of an uncharged drop being a straight vertical line. In a particular arrangement of actual apparatus, the parallel deflection plates are 3.10 m long vertically and spaced .018 m apart. Potentials up to 100 Kv DC are available to produce the electric field for deflecting the drops. The deflection in the x-direction (parallel to the electric field) is given by

$$x = \frac{qEv_o^2}{mg^2} \left( 1 + \frac{Lg}{v_o^2} - 1 + \frac{2Lg}{v_o^2} \right) \tag{1}$$

where $q$ is the charge on the drop whose mass is $m$, $E$ is the electric field in the x-direction, $v_0$ is the initial vertical velocity of the drop (in the z-direction), $L$ is the length of the deflection field in the z-direction, and $g$ is the acceleration due to gravity.

For example, a 30 micrometer diameter drop of fluid with a density of 1.0 gm/cc, an initial vertical velocity of 10 meters/sec., and carrying a net charge of $1.6 \times 10^{-19}$ coulombs (one electron) will be deflected transversely a distance 0.71 mm by a field of $1.67 \times 10^{6}$ volts/meter in the 3.1 meter long plate system. Thus, such drops whose net charge differs by $\pm$ 1 electron will be separated a distance of .71 mm. Equation (1) results from the integration of the equations of motion for a drop falling vertically between vertical, parallel plates with the following conditions:

$$x = y = z = 0 \qquad \text{at } t = 0$$

$$v_x = v_y = 0 \qquad \text{at } t = 0$$

$$v_z = v_0 \qquad \text{at } t = 0$$

The deflection plates are in the $x = -\frac{d}{2}$, $y$, $z$, and $x = +\frac{d}{2}$, $y$, $z$ planes and the plates are maintained at potentials of $\frac{V}{2}$ and $-\frac{V}{2}$ such that the electric field has only an x component, i.e., $E_x = \frac{V}{d}$, $E_y = E_z = 0$. The plate length is $L$ and the width is $w$. The drop radius is $a$ and its mass is $m = \frac{4}{3} \pi a^3 \rho$ where $\rho$ is the liquid density. The drop carries a charge $q$ and the $g$ is the acceleration due to gravity.

Equation (1) is correct if the drops are very far apart in a vertical line and are freely falling in a vacuum. There are several terms which make up the total electrical force on a drop in the space between two electrified plates.

$$F = F_{qE} + F_{im} + F_{qq} + F_{D} + F_{Ho}$$

The first term $F_{qE}$ results from the interaction of an applied electric field E on the net charge q carried by the drop and is given by $F_{qE} = qE$. The second force $F_{im}$ results from the interaction of the charge q on a drop and its image charge $q_{im}$ in any nearby material such as the conducting deflection plates or even other drops. This force has the form $F_{im} = \dfrac{q\, q_{im}}{4\pi\epsilon_o (2R)^2}$ where q is the drop charge and 2R is the distance between the charge q and its image $q_{im}$. For charges of a few electrons and spacings of at least a few tens of micrometers, the image forces are about three to five orders of magnitude less than the $F_{qE}$. Similarly the force $F_{qq}$ between drops due to each of their respective net charges is three to five orders of magnitude less than $F_{qE}$. The force between drops as the result of induced positive and negative charges on the drops by the electric field may be larger than $F_{qE}$ in some situations. This force, $F_D$, the dipole force will be considered in more detail in following paragraphs. The forces labeled $F_{HO}$ are those forces owing to higher order multipole terms. These higher order force terms are many orders of magnitude lower than even the image forces and can be ignored compared to $F_{qE}$ and $F_D$. Because the drops are falling in a vacuum, gas dynamic forces can be ignored.

If the drops are close together, but start downward into the electric field along the same trajectory, Eq. (1) should be modified to account for the interdrop forces resulting from polarization charges produced by the electric field.

If a material sphere is put into a uniform electric field E, polarization charges appear at the surface of the sphere. In effect, the sphere becomes a dipole as shown in Fig. 2. The electric field will produce polarization charges on the surface of the sphere where the charge per unit area is $\sigma = \frac{3K\epsilon_0}{K+2} E \cos \Theta$. The applied electric field is E, $\Theta$ is the polar angle with the direction of the polar axis along the applied electric field and K is the dielectric constant (assuming the sphere is a nonconducting dielectric). This result is obtained by straight forward solution of Laplace's equation in spherical polar coordinates for a dielectric sphere immersed in a uniform electric field with appropriate boundary conditions. A surface integration over the hemispheres, $0 \leq \Theta \leq \frac{\pi}{2}$ and $\frac{\pi}{2} \leq \Theta \leq \pi$ gives the charge on each hemisphere to be

$$Q = \frac{3\pi\ KE_0}{K+2}\ Ea^2$$

where a is the radius of the sphere. An integration of the moment of the charge allows us to find the centroid of charge for each hemisphere which a distance is $\frac{2a}{3}$ from the center of the sphere along the polar axis. Thus, the sphere is a good approximation to a monopole q at the center of the sphere and a dipole with a length $\frac{4a}{3}$ and dipole charge of $Q = \frac{3\pi KE_0}{K+2}\ Ea^2$. As was mentioned earlier, the higher order multipole terms are ignored because the forces produced by those terms are several order of magnitude smaller than the monopole and dipole terms.

## II. THEORY

Consider a set of three drops, A, B, and C, as shown in Fig. 2. The force, $F_B$ in the x-direction on the middle drop due to the polarization charges is given by

$$F_B = 2\left(\frac{Q^2}{4\pi\epsilon_0 D^2}\right) \frac{2\zeta}{[\zeta^2 + \ell^2]^{3/2}} + \frac{1-\zeta}{[(1-\zeta)^2 + \ell^2]^{3/2}} - \frac{1+\zeta}{[(1+\zeta)^2 + \ell^2]^{3/2}} \qquad (2)$$

where $Q = \frac{3\pi\epsilon_0 k}{k+2} Ea^2$ is the dipole charge, $D = \frac{4a}{3}$ is the dipole length, $x_B = \zeta D$ is the displacement of drop B with respect to a line between drops A and C, $s = \ell D$ is the vertical, center-to-center spacing between the drops, and a is the drop radius. The force $F_B$ on drop B owing to the presence of polarization charges is found by replacing the drops by positive and negative point charges spaced as discussed in the previous paragraphs and determining the force by simple application of Coulomb's Law. This force is similar to the force between dipoles except for the macroscopic separation of the positive and negative induced charges. A true dipole has a length which approaches zero and a charge such that $q\ell$ is finite and equal to the dipole moment.

The x-component of the electric field at drop B arising from the dipoles of drops A and C is several orders of magnitude less than the applied field E. Therefore, even though it is opposite in direction to the applied field, no significant depolarization effect occurs. That is, the magnitudes of the polarization charges are virtually unaffected by the fields other polarized drops.

Getting back to Eq. (2), one observes that for small displacements the force $F_B$ is in the direction of the displacement $\zeta$ thus qualifying itself as a destabilizing force. Also, if one is interested in gaining some insight into the force $F_B$ as to its possible effects on the behavior of the middle drop B, a small-displacement-expansion of $F_B$ can be made assuming that $\zeta \ll \ell$. The net result is an equation of motion for the displacement $\zeta$, which is

$$d^2\zeta(t)/dt^2 = 2G\zeta(t) \tag{3}$$

where G is positive constant characterizing the strength of the force on the drop B due to the drops A and C, and is a function of the dipole charge and length Q and D, the drop mass m, the vertical, center-to-center spacing between the drops $\ell$, and the free space permittivity $\epsilon_0$.

A general solution to Eq. (3) is

$$\zeta(t) = 1/2\ [\zeta(0) - \beta\zeta(0)]\ e^{-t/\beta} + 1/2[\zeta(0) + \beta\zeta(0)]\ e^{t/\beta} \tag{4}$$

where $\zeta(0)$ and $\zeta(0)$ are, respectively, the initial values of $\zeta(t)$ and its time derivative $d\zeta(t)/dt$, and $\beta = 1\ /\ 2G$ is a characteristic time over which the drop B reacts to the force $F_B$, displacing itself from the original position. For the conditions, under which the present experiments were carried out, $\zeta(0) \gg \beta\zeta(0)$, thus simplifying Eq. (4) to:

$$\zeta(t) = \zeta(0)\ \cosh(t/\beta) \tag{5}$$

where $\beta$ is on the order of a millisecond. One can also show that for large $\ell(\geq 6)$, $\beta \propto \ell^{5/2}$.

## III. Experiment

Experimentally the effects of the induced charges become apparent in the deflections of drops with equal masses whose net charges differ by integer numbers of electrons. By Eq. (1) we see that the differences in the deflections of any two drops with charges differing by one electronic charge should be the same. However, we see experimentally that the deflection differences are not always the same for one electronic charge difference.

To observe the deflection of the drops by the action of the field between the parallel plates as shown in Fig. 1, a camera is placed at the bottom of the deflection plates. The optical axis of the camera is directed perpendicular to the direction of the electric field and horizontally. That is, the camera "looks" at the spread of the drops coming out from between the deflection plates. The drops are illuminated by a sheet beam of light from an argon ion laser located below the field of view of the camera and on the opposite side of the deflection plates from the camera. The beam is directed up at an angle of about 30 degrees from the horizontal so the light does not shine directly into the camera lens. Thus, only specularly reflected light from the drops enters the camera lens as the drops pass vertically downward through the sheet of laser light. Each drop leaves a vertical streak on the film as it goes downward through the light beam. The multiple vertical streaks shown in Fig. 3 are from about 300 drops seen by the camera during a shutter open time of 0.01 second. The drops are spread horizontally according to the number of electron (+ or -) carried by each drop. In the absence of dipole forces, all the spacings between the drops (streaks) would be multiples of some least space (0.09 mm) corresponding to a charge difference of one electron between two drops.

This is shown in Fig. 3 where the most closely spaced vertical lines are trajectories of drops whose net charge differs by one electron. The streaks on the photograph in Fig. 3 are in effect extensions of the trajectories shown in Fig. 1. Note that the horizontal spacing in Fig. 1 is exaggerated. The plate length in the experiment is 3.1 meters and the plate spacing is only 0.018 meters, so the drops are still traveling almost vertically as they exit the space between the plates. Because of the drop-drop interactions resulting from the polarization charges, the trajectory spacings are not all integer multiples of a least value of deflection for one electron. The drops which produced the lines, shown in Fig. 3, initially entered the deflection field spaced approximately two diameters apart vertically. If we compare the forces resulting from the electric field acting on the net charge with the forces resulting from polarized charge interactions, we see that a spacing of 20 diameters between drops would reduce the interactive forces to a reasonable value. Such spacing may be accomplished by removing 9 out of 10 drops in the stream. Several methods are available to effect the removal of the unwanted drops.

If the 9 drops to be removed were highly charged, an electric field could be used to deflect the charged drops into a collector, leaving the remaining, virtually uncharged, drops to continue on through the main deflection field. Because the drops are formed from a high resistivity liquid ($\rho \geq 10^{14}$ ohm-centimeters), inductive charging during the formation process is difficult. To circumvent this problem a pulsed electron beam can be used to charge the drops which are to be removed. By pulsing the electron beam off at appropriate times, every tenth drop can be left uncharged. Preliminary experiments have provided some encouraging results.

However, a method has been devised to generate drops less than 30 micrometers in diameter, but spaced by several hundred micrometers. This requires no charging of the drops and produces exceptionally stable streams of drops. Further experiments must be conducted to assess the efficiency of this method of producing virtually isolated drops.


## ACKNOWLEDGEMENT

The authors would like to thank Tom Kuklo for his assistance in the experimental phase of this work.


## REFERENCES


1. A. F. Hebard and W. M. Fairbank, "Search for Fractional Charge (Quarks) Using a Low Temperature Technique," Proc. 12th Int. Conf. Low Temp. Phys., Kyoto (Tokyo, Keigaku Publishing Co., 1970).

2. G. Hirsch, R. Hagstrom, and C. Hendricks, "A Sensitive Method for Detecting Stable Fractional Charges on Matter," Lawrence Berkeley Laboratory Report LBL-9350, UC-349, June 1979.


2051H

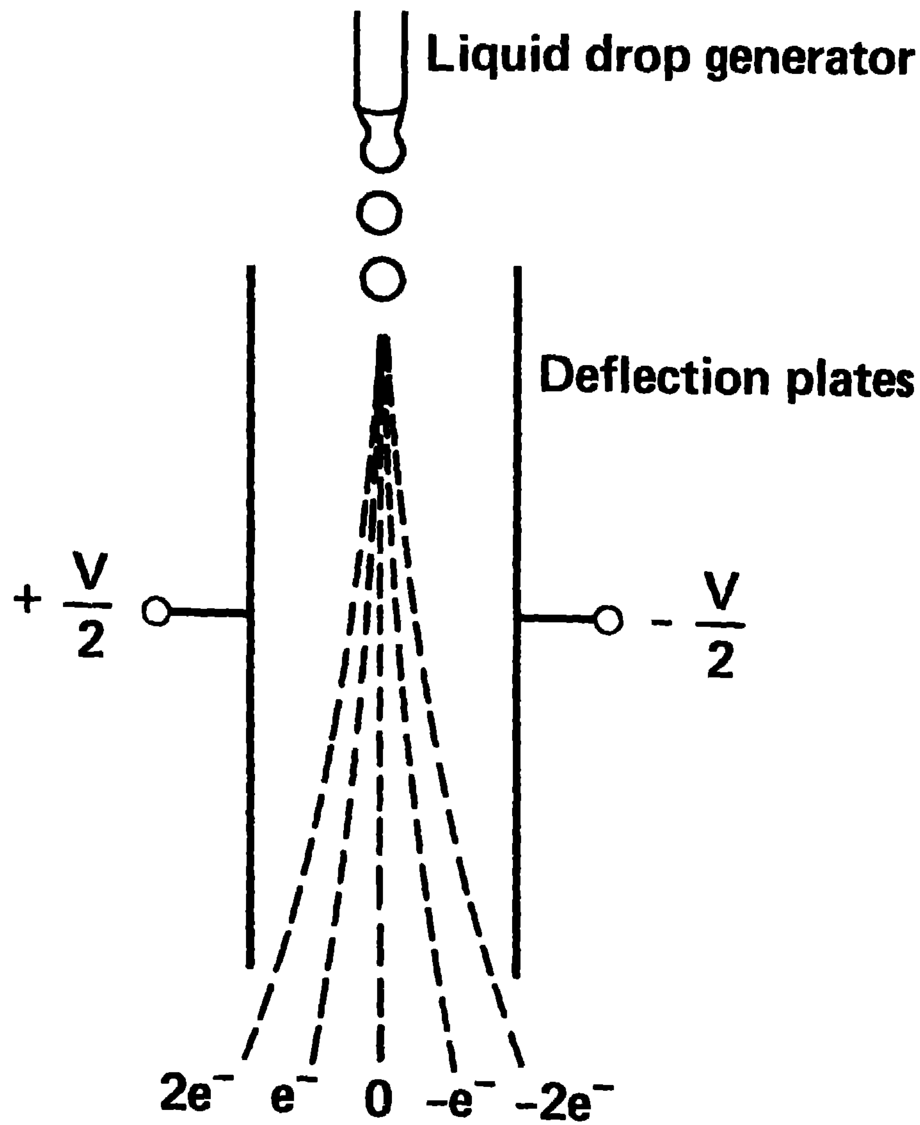


Figure 1

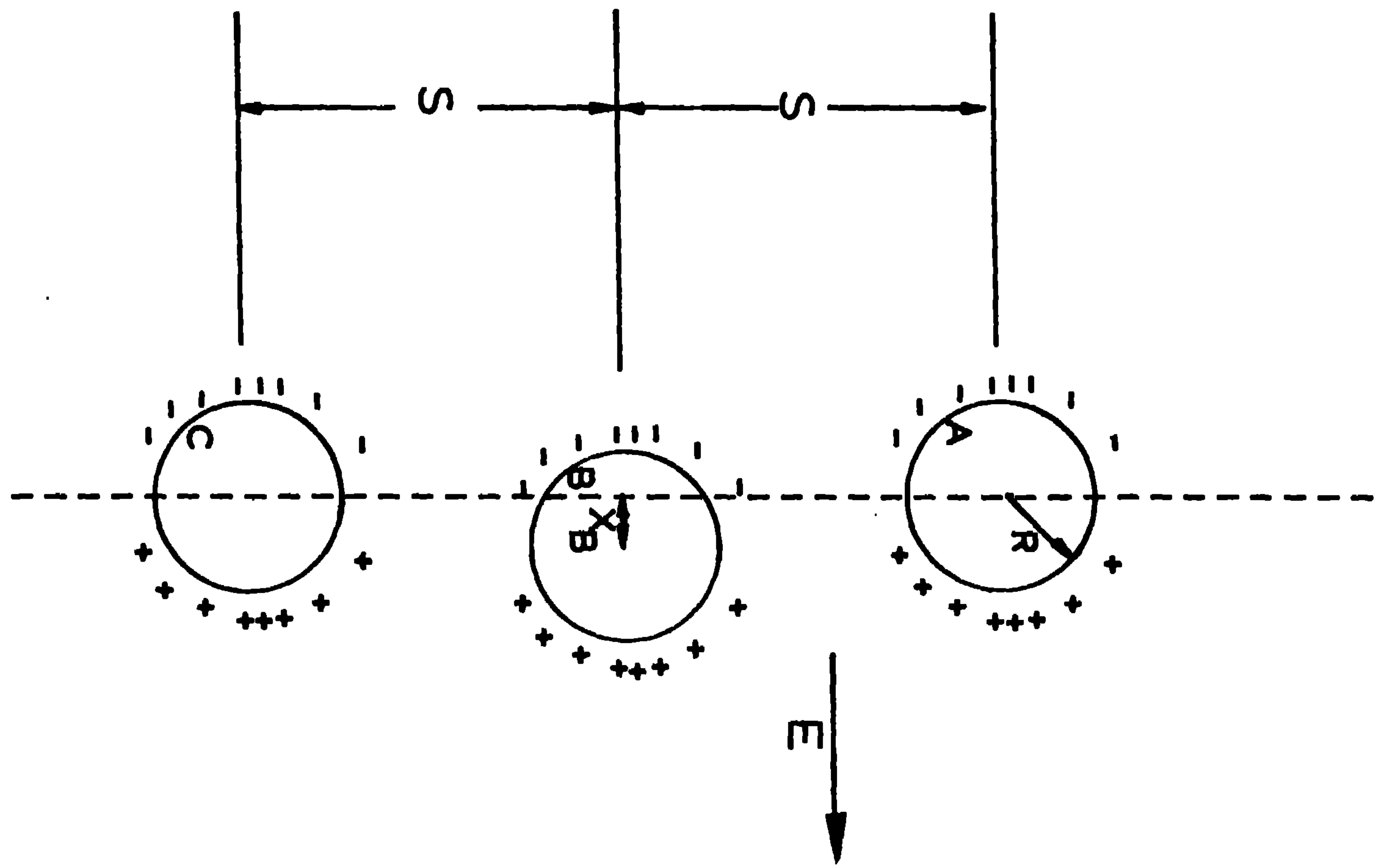


Figure 2

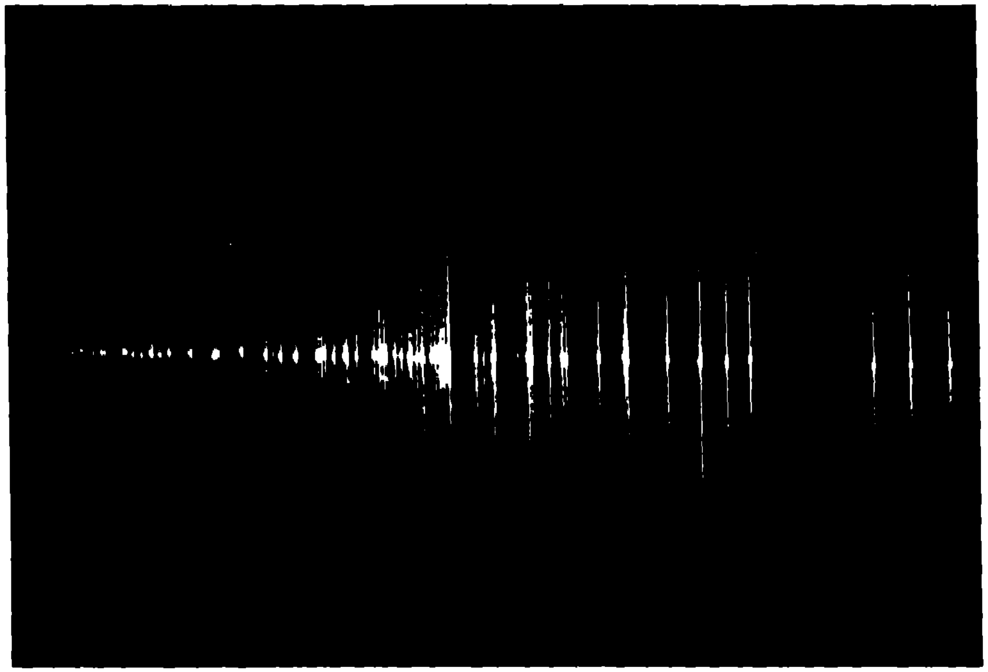

| | |
|---|---|
| Drop diameter | 100 $\mu$m |
| Liquid density | 934 kg/$m^3$ |
| Initial velocity | 2.5 m/sec |
| E-field | $1.67 \times 10^6$ V/m |
| Deflection plates | |
| Length | 3.1 m |
| Spacing | 1.8 cm |

Figure 3